Princeton Plasma Physics Laboratory

PPPL-5368

Conductivity tensor for anisotropic plasma in gyrokinetic theory

P. Porazik and J. R. Johnson

March 2017

Prepared for the U.S.Department of Energy under Contract DE-AC02-09CH11466.

Princeton Plasma Physics Laboratory
Report Disclaimers

Full Legal Disclaimer

Trademark Disclaimer

PPPL Report Availability

Princeton Plasma Physics Laboratory:

http://www.pppl.gov/techreports.cfm

Office of Scientific and Technical Information (OSTI):

http://www.osti.gov/scitech/

Related Links:

U.S. Department of Energy

U.S. Department of Energy Office of Science

U.S. Department of Energy Office of Fusion Energy Sciences

Conductivity tensor for anisotropic plasma in gyrokinetic theory.

Peter Porazik[1, a)] and Jay R. Johnson[1, b)]

Princeton Plasma Physics Laboratory, Princeton University, Princeton, New Jersey, 08542, USA

(Dated: 28 February 2017)

It has been argued that the oblique firehose and mirror instabilities are important candidates for regulation of temperature anisotropy in the solar wind. To quantify the role of anisotropy driven instabilities, global kinetic simulations of the solar wind would be extremely useful. However, due to long time scales involved, such simulations are prohibitavely expensive. Gyrokinetic theory and simulations have proven to be valuable tools for the study of low frequency phenomena in nonuniform plasmas, however there are discrepencies between the anisotropy driven instabilities appearing in the gyrokinetic theory and those of a fully kinetic one. We present a derivation of the conductivity tensor based on the arbitrary frequency gyrokinetics, and show that relaxing the condition that $\omega/\Omega \ll 1$, where ω is the wave frequency, and the Ω is the cyclotron frequency, eliminates these discrepencies, while preserving the advantages of the gyorkinetic theory for global kinetic simulations.

[a)]Electronic mail: pporazik@pppl.gov

[b)]Electronic mail (corresponding author): jrj@andrews.edu; Now at:Andrews University, 8450 E Campus Circle Dr, Berrien Springs, Mitchigan, 49103, USA

I. INTRODUCTION

Recently it has been shown that anisotropy driven instabilities, especially the firehose and mirror type, are important candidates for the regulation of temperature anisotropy in the solar wind[1,15,17]. Valuable insights into underlying mechanisms of these regulating processes may be gained via computer simulations. Athough fluid simulation models are sufficiently fast to capture the global nature of the problem, they lack the ability to resolve the equally essential kinetic physics. For this reason, fully kinetic simulations are commonly employed to investigate the behavior of these instabilities, e.g. *Gary*[8], *Seough et al.*[34], *Yoon et al.*[41]. However, when the phenomena of interest are much slower than the cyclotron period of the simulated species, fully kinetic simulation models can overwhelm the computational resources by computing unnecessary details. Although hybrid simulations, with fully kinetic ions and massless fluid electrons[4,12–14], are frequently employed to balance these two extremes, in the case of oblique firehose and mirror instabilities the time scales of interest are still much longer that the ion cyclotron period, motivating an inquiry into a more efficient simulation model.

Gyrokinetic simlulations are currently the most important tool for global studies of low frequency kinetic phenomena in fusion plasmas, i.e. phenomena whose time scales are longer than the cyclotron period; and they are becoming more common in the studies of space and astrophysical plasmas[7,23–25,27,32,39]. However, the gyrokinetic theory, and corresponding simulation codes, generally assume that $k_\parallel \ll k_\perp$, i.e. the wavelength of perturbations along the magnetic field line is much longer than perpendicular to it[3]. As it turns out, the most unstable Alfvenic perturbations in fusion devices indeed satisfy this criterion, which represents minimum bending of the magnetic field lines. However, temperature anisotropy modifies the relative importance of the stabilizing effect of the field line bending, and the high β anisotropy driven instabilities such as the mirror and the oblique firehose are most unstable when $k_\parallel \approx k_\perp$, while $k_\perp \rho \sim 1$ is still valid (β is the ratio of plasma pressure to magnetic pressure, ρ is the Larmor radius,and the directions of k-vectors are relative to the magnetic field). Consequently, a simulation model based on a gyrokinetic theory which does not take this into account will result in their incomplete description. For example, the growth rate for the mirror instability will not capture the stabilization at large $k_\parallel$, i.e. the field line bending eventually has to stabilize the mode; and the oblique firehose,

will be completely missed. However, the advantage of the gyrokinetic theory results from the decoupling of the gyro-motion from the rest of the particle dynamics, and not from the frequency ordering, or the related $k_\parallel \ll k_\perp$ assumption[28]. As has been shown using the gyrocenter phase space transformations, such decoupling can be accomplished without the requirement that these conditions be satisfied, and corresponding efficient gyrokinetic simulations can still be designed[19,20,31].

The gyrokinetic theory has been initially extended to arbitrary frequencies by *Brizard*[2], *Chen and Tsai*[5], *Chiu*[6], *Lee et al.*[22]. Later it was reformulated in terms of the generating function of phase space transfromations, the gyro-gauge function, by *Qin*[28], who then used the approach to show how the fast compressional Alfven wave may be reintroduced into the gyrokinetic theory, and the ideal MHD may be recovered from it[28,30]. The formulation of the gyrokinetic theory in terms of phase space transformations enable one to systematically decouple the particle's gyro-motion from the rest of its dynamics. This is the key advantage of the formulation, and what makes it suitable for efficient computer simulations. The approach has been shown to reduce computation time in particle-in-cell simulations even in cases when the time scales of the order of the cyclotron period are important to consider, such as RF heating[16,21,42].

In this manuscript we use the arbitrary frequency gyrokinetic kinetic theory, or the gyro-gauge kinetic theory, and outline the derivation of the gyrokinetic conductivity tensor for an anisotropic plasma, without assuming that the wave frequency is much less than the cyclotron frequency, or $k_\parallel \ll k_\perp$. We then numerically solve thus obtained dispersion relation for the mirror instability and the oblique firehose instability, and compare the results with solutions obtained using the fully kinetic conductivity tensor[12,18]. The motivation is to demonstrate that the key instabilities that regulate the anisotropy in the solar wind may be correctly recovered using this approach, which can therefore be used as the basis of an efficient global simulation model for the study of the solar wind.

II. PRELIMINARY CONSIDERATIONS

In this section we outline the derivation of the conductivity tensor. After stating our working assumptions, we discuss the relationship between the fields $(\delta\phi, \delta A_\parallel, \delta B_\parallel)$, in terms of which the current in gyrokinetic theory is expressed, and the electric field components

(E_x, E_y, E_z). Once the expression for the gyrokinetic current is obtained, this relationship may be used to find the conductivity tensor components.

For simplicity we assume a two component plasma with bi-Maxwellian ions and Maxwellian electrons,

$$F_{i0} = n_0 \sqrt{\frac{m_i}{(2\pi)^3 T_{i\parallel} T_{i\perp}^2}} e^{-\left(\frac{m_i v_\parallel^2}{2T_{i\parallel}} + \frac{\mu B_0}{T_{i\perp}}\right)}, \tag{1}$$

$$F_{e0} = n_0 \sqrt{\frac{m_e}{(2\pi T_e)^3}} e^{-\left(\frac{m_e v_\parallel^2}{2} + \mu B_0\right)/T_e}, \tag{2}$$

where m_s is the particle mass of species s, $v_\parallel$ is the component of the velocity parallel to the magnetic field; B_0 is the magnitude of the background magnetic field; μ is the magnetic moment, given by $m_s v_\perp^2 / 2B_0$, for species s; $v_\perp$ is the magnitude of the velocity perpendicular to the background magnetic field; T_e is the electron temperature, which is assumed to be isotropic; $T_{i\parallel}$ and $T_{i\perp}$ are the parallell and perpendicular temepratures of ions;

In this section we use the following normalizations: time is normalized to the cyclotron period $\Omega_i^{-1} = m_i c / eB_0$, space to the proton Larmor radius $\rho_i = \sqrt{T_{i\perp}/m_i}/\Omega_i$, magnetic field to B_0, and electric field to $T_{i\perp}/e\rho_i$. Here, c is the speed of light, e is the proton charge, m_i is the proton mass, $T_{i\perp}$ is the temperature of ions perpendicular to magnetic field, and B_0 is the background magnetic field. The background magnetic field is assumed to be uniform and along the z-axis, which therefore corresponds to the "parallel" direction; the "perpendicular" direction is along the x-axis.

The normalized wave equation may be written as,

$$\mathbf{k} \times \mathbf{k} \times \mathbf{E} + \frac{\omega^2}{c^2}\mathbf{E} + i\omega \frac{\beta_{i\perp}}{2}\mathbf{J} = 0, \tag{3}$$

$$\mathbf{J} = \sum_s \boldsymbol{\sigma}_s \cdot \mathbf{E} = -\frac{2i\omega}{\beta_{i\perp} c^2} \sum_s \boldsymbol{\chi}_s \cdot \mathbf{E}, \tag{4}$$

where the the index of the sum corresponds to species s,and $\beta_{i\perp}$ is the radio of kinetic pressure to magnetic pressure, explicitly given by $4\pi n_0 T_{i\perp}/B_0^2$. In gyrokinetic theory, the electromagnetic fields are expressed in terms of the scalar potential ($\delta\phi$), the compressional component of magnetic field perturbation ($\delta B_\parallel$) and the magnitude of the vector potential in the parallel direction ($\delta A_\parallel$)[3]. In terms of these quantities, the electric field is (using above

normalizations)

$$E_x = -ik_\perp \delta\phi - i\omega \frac{k_\parallel}{k_\perp} \delta A_\parallel, \tag{5}$$

$$E_y = \frac{\omega}{k_\perp} \delta B_\parallel, \tag{6}$$

$$E_z = -ik_\parallel \delta\phi + i\omega \delta A_\parallel, \tag{7}$$

in the Coulomb gauge ($\nabla \cdot \mathbf{A} = 0$). The above transformation equations can be written as

$$\mathbf{E} \equiv \begin{bmatrix} E_x \\ E_y \\ E_z \end{bmatrix} = \underbrace{\begin{bmatrix} -ik_\perp & -i\omega\frac{k_\parallel}{k_\perp} & 0 \\ 0 & 0 & \frac{\omega}{k_\perp} \\ -ik_\parallel & i\omega & 0 \end{bmatrix}}_{\mathbf{G}} \underbrace{\begin{bmatrix} \delta\phi \\ \delta A_\parallel \\ \delta B_\parallel \end{bmatrix}}_{\mathbf{E}'} \equiv \mathbf{G}\mathbf{E}'.$$

Then, using Eq. 4, the current can be written in terms of $\mathbf{E}'$ as

$$\mathbf{J} = \sum_s \boldsymbol{\sigma}_s \cdot \mathbf{E} = \sum_s \boldsymbol{\sigma}_s \cdot \mathbf{G}\mathbf{E}' = \sum_s \boldsymbol{\sigma}'_s \cdot \mathbf{E}'. \tag{8}$$

The explicit expression for current is found from the gyrokinetic equation, and is therefore in terms of $\boldsymbol{\sigma}'_s$ and $\mathbf{E}'$. The corresponding conductivity tensor is

$$\boldsymbol{\sigma}_s = \boldsymbol{\sigma}'_s \mathbf{G}^{-1}, \tag{9}$$

where

$$\mathbf{G}^{-1} = \begin{bmatrix} \frac{ik_\perp}{k^2} & 0 & \frac{ik_\parallel}{k^2} \\ \frac{ik_\parallel k_\perp}{\omega k^2} & 0 & -\frac{ik_\perp^2}{\omega k^2} \\ 0 & \frac{k_\perp}{\omega} & 0 \end{bmatrix}.$$

In this manner a clear comparison between the matrix elements obtained from the fully kinetic theory and the gyrokinetic theory can be made.

III. OBTAINING THE CURRENT

The gyrokinetic equation determines the ion gyrocenter distribution function, designated by δF_i, and related to the particle distribution function by

$$\delta f_i(\mathbf{z}, t) \approx e^{-\boldsymbol{\rho}\cdot\nabla} \delta F_i(\mathbf{Z}, t)|_{\mathbf{z}} + e^{\boldsymbol{\rho}\cdot\nabla} \delta\mathbf{Z} \cdot e^{\boldsymbol{\rho}\cdot\nabla} \partial_{\mathbf{Z}} F_{i0}(\mathbf{Z}, t)|_{\mathbf{z}} \tag{10}$$

where $\mathbf{z} \equiv (\mathbf{x}, \mathbf{v})$, and $\mathbf{Z} \equiv \left(\mathbf{X}, v_\parallel, \mu, \xi\right)$ are guiding center variables

$$\begin{aligned} \mathbf{X} &\equiv \mathbf{x} - \boldsymbol{\rho} \\ v_\parallel &\equiv \hat{\mathbf{b}} \cdot \mathbf{v} \\ \xi &\equiv \tan^{-1} \hat{1} \cdot \mathbf{v} / \hat{2} \cdot \mathbf{v} \end{aligned} \tag{11}$$

corresponding to the guiding center position ($\mathbf{X}$), parallel velocity ($v_\parallel$), magnetic moment (μ), and phase angle (ξ), respectively. The Larmor radius is defined by $\boldsymbol{\rho} = \Omega_i^{-1} \hat{\mathbf{b}} \times \mathbf{v}_\perp = \rho_\perp \left(\hat{1} \cos\xi + \hat{2} \sin\xi\right)$, where$\rho_\perp \equiv v_\perp \Omega_i$, and $(\hat{1}, \hat{2}, \hat{\mathbf{b}})$ is an orthogonal triad of unit vectors which in our case correspond to $(\hat{\mathbf{x}}, \hat{\mathbf{y}}, \hat{\mathbf{z}})$. Treating only ions gyrokinetically, for simplicity, and with the above considerations, the perturbed current may be written as,

$$\begin{aligned} \mathbf{J} =& \int \mathbf{v} \delta f_i d\mathbf{v} - \int \mathbf{v} \delta f_e d\mathbf{v}. \\ =& \int e^{-i\sqrt{2\lambda\mu}\cos\xi} \left(\hat{\mathbf{z}} v_\parallel - \hat{\mathbf{y}} \sqrt{2\mu} \cos\xi - \hat{\mathbf{x}} \sqrt{2\mu} \sin\xi\right) \left(\delta F_i + \delta v_\parallel \partial_{v_\parallel} F_{i0} + \delta\mu \partial_\mu F_{i0}\right) \Big|_{\mathbf{z}} dv_\parallel d\mu d\xi \\ & - \int \mathbf{v} \delta F_e d\mathbf{v}, \end{aligned} \tag{12}$$

where the λ parameter is given by $k_\perp^2 \rho_i^2$ in unnormalized units, and

$$\delta F_i = -\left[\left(\delta\phi - s\delta A_\parallel\right) J_0\left(\sqrt{2\lambda\mu}\right) + \mu \delta B_\parallel \frac{2}{\lambda\mu} J_1\left(\sqrt{2\lambda\mu}\right)\right] \left(1 - \frac{s}{s - v_\parallel}\right) F_{0i}, \tag{13}$$

$$\delta v_\parallel = \delta A_\parallel J_1\left(\sqrt{2\lambda\mu}\right) 2i\cos\xi + ik_\parallel S, \tag{14}$$

$$\delta\mu = \mu\delta B_\parallel \frac{2}{\sqrt{2\lambda\mu}} \left\{-J_1\left(\sqrt{2\lambda\mu}\right) + \left[J_0\left(\sqrt{2\lambda\mu}\right) - \frac{1}{\sqrt{2\lambda\mu}} J_1\left(\sqrt{2\lambda\mu}\right)\right] 2i\cos\xi\right\} + \partial_\xi S, \tag{15}$$

where $s = \omega/k_\parallel$, and $S = S(v_\parallel, \mu, \xi)$ is the gyro-gauge function, which contains all the details of the transformation between particles and gyrocenters, as will be later discussed. δF_i represents the linear response of the gyrokinetc distribution function of ions; $\delta v_\parallel$ corresponds to the modification of the parallel velocity of ions due to the perturbation; and $\delta\mu$ corresponds to the modification of the magnetic moment of ions due to the perturbation. Both, $\delta v_\parallel$ and $\delta\mu$, depend on the gyrogauge function S, which essentially defines their meaning. The reader is referred to[28,29] for more details. Eq. 12 determines the dependence of $\mathbf{J}$ on the field quantities $(\delta\phi, \delta B_\parallel, \delta A_\parallel)$. From it, the elements of $\boldsymbol{\sigma}_s'$ may be found, and used to compute the conductivity tensor, and the susceptibility tensor $\boldsymbol{\chi}_s$.

The gyro-gauge function plays the central role in gyrokinetic theory, containing all the details of the transformation between particles and gyrocenters[28]. It is the generating function for the transformation between the two, and thus it determines how the gyro-motion is decoupled from the particle motion. This decoupling is the reason why gyrokinetic simulations can provide significant advantage over the fully kinetic schemes. The gyro-gauge function is the solution to[28]

$$\left(\partial_t + v_\parallel \hat{\mathbf{b}} \cdot \partial_{\mathbf{X}} + \partial_\xi\right) S = \widetilde{\delta\phi} - \widetilde{\mathbf{v} \cdot \delta\mathbf{A}}, \tag{16}$$

where

$$\widetilde{\delta\phi} = \left[e^{i\sqrt{2\lambda\mu}\cos\xi} - J_0\left(\sqrt{2\lambda\mu}\right)\right]\delta\phi, \tag{17}$$

$$\widetilde{v_\parallel \delta A_\parallel} = \left[e^{i\sqrt{2\lambda\mu}\cos\xi} - J_0\left(\sqrt{2\lambda\mu}\right)\right]\delta A_\parallel v_\parallel, \tag{18}$$

$$\widetilde{\mathbf{v}_\perp \cdot \delta\mathbf{A}_\perp} = \left[\frac{2i}{\sqrt{2\lambda\mu}} e^{i\sqrt{2\lambda\mu}\cos\xi}\cos\xi + \frac{2}{\sqrt{2\lambda\mu}} J_1\left(\sqrt{2\lambda\mu}\right)\right]\mu\delta B_\parallel, \tag{19}$$

which corresond to oscillatory components of the field quantities. The solution is,

$$S = -\sum_{n\neq 0} \frac{i\left(\delta\phi - v_\parallel \delta A_\parallel\right)}{n + k_\parallel v_\parallel - \omega} i^n J_n e^{in\xi} - \sum_{n\neq 0} \frac{2}{\sqrt{2\lambda\mu}} \frac{\mu\delta B_\parallel}{n + k_\parallel v_\parallel - \omega} i^{n-1} J_n' e^{in\xi}. \tag{20}$$

Any approximations of Eq. 20 determine how much of the detail of particle motion is retained. For example, standard gyrokinetics is obtained when S is expanded assuming that $\omega \ll \Omega_i$, and only the lowest order in ω/Ω_i is kept. Instead of transforming to the Fourier space to obtain Eq. 20, in gyrokinetic particle simulations, Eq. 16 may be treated as other phase-space variables and integrated in time[21]. For simplicity of expression, we keep only the $n = \pm 1$ components, removing higher order cyclotron resonances,

$$\begin{aligned} S = &\left(\delta\phi - v_\parallel \delta A_\parallel\right) J_1 \left(\frac{e^{i\xi}}{k_\parallel v_\parallel - \omega + 1} + \frac{e^{-i\xi}}{k_\parallel v_\parallel - \omega - 1}\right) \\ &- \frac{2\mu\delta B_\parallel}{\sqrt{2\lambda\mu}} \left(J_0 - \frac{1}{\sqrt{2\lambda\mu}} J_1\right) \left(\frac{e^{i\xi}}{k_\parallel v_\parallel - \omega + 1} + \frac{e^{-i\xi}}{k_\parallel v_\parallel - \omega - 1}\right) \end{aligned} \tag{21}$$

The first integral in Eq. 12 can be written as a sum of two contributions, one coming from the guiding center distribution function δF_i, which can be designated by $\mathbf{J}^{\delta F}$, and the other coming from finite Larmor radius (FLR) corrections, which can be designated by $\mathbf{J}^{FLR}$. Combining Eq. 12 with Eq. 20 the following expressions for the components of $\mathbf{J}^{\delta F}$

are obtained,

$$J_x^{\delta F} = 0, \tag{22}$$

$$J_y^{\delta F} = -\frac{i\sqrt{\lambda}e^{-\lambda}}{2T_{i\|}}(\delta A_\| s - 2\delta B_\| - \delta\phi)(-I_0 + I_1)\left(\frac{s}{\sqrt{2T_{i\|}}}Z + 1\right)\beta_i, \tag{23}$$

$$J_z^{\delta F} = \frac{e^{-\lambda}s}{2T_{i\|}}\left(\left[\delta A_\| s - \delta B_\| - \delta\phi\right] I_0 + \delta B_\| I_1\right)\left(\frac{s}{\sqrt{2T_{i\|}}}Z + 1\right)\beta_i. \tag{24}$$

The components of $\mathbf{J}^{FLR}$ are equally straightforward, but due to their length were placed in the Appendix. The elements of $\boldsymbol{\sigma}'_s$ can be directly read from these expressions for current, and the conductivity tensor may then be found using Eq. 9.

IV. APPLICATION TO MIRROR AND OBLIQUE FIREHOSE

The mirror instability[10,35,38] is a kinetic instability which results when

$$2 - \sum_s \beta_{s\perp}\left(\frac{T_{s\|}}{T_{s\perp}} - 1\right) < 0. \tag{25}$$

A gyrokinetic set of equations has been previously used to analyze the mirror instability, however these derivations were based on the low frequency version of the gyrokinetic theory, in which the terms of order $k_\| v_\|/\Omega_i$ are treated as small and are systematically neglected. The neglect of the higher order terms results in a dispersion relation in which $k_\|$ enters only as a scaling factor of ω, so that the growth rate is linearly proportional to $k_\|$. Not only is such a description of the mirror instability incomplete, a simulation model based on it would produce grid-scale instabilities. To recover the stabilization at high $k_\|$ the previous derivations thus introduce higher order terms into the perpendicular Ampere's law ad hoc[26,32,33]. Here we obtain the correct behavior of the mirror instability by working systematically with the gyro-gauge function, the gyrokinetic equation, and the Maxwell's equations. The result is shown in the left panel of Figure 1, for ion parameters $R = T_{i\perp}/T_{i\|} = 6$, $\beta_\perp = 4\pi n_0 T_{i\perp}/B_0^2 = 0.43$, and $c/\sqrt{T_{i\perp}/m_i} = 10^3$. The electrons are isotropic with $T_e/T_i = 10^{-4}$. The growth rate agrees with the fully-kinetic derivation, shown in the right panel, for comparison. In both cases, the stabilization at large $k_\|$ is clearly displayed.

The oblique firehose instability has been first investigated in detail by *Hellinger and Matsumoto* [12], while many of its essential features were captured earlier by *Yoon et al.* [40].

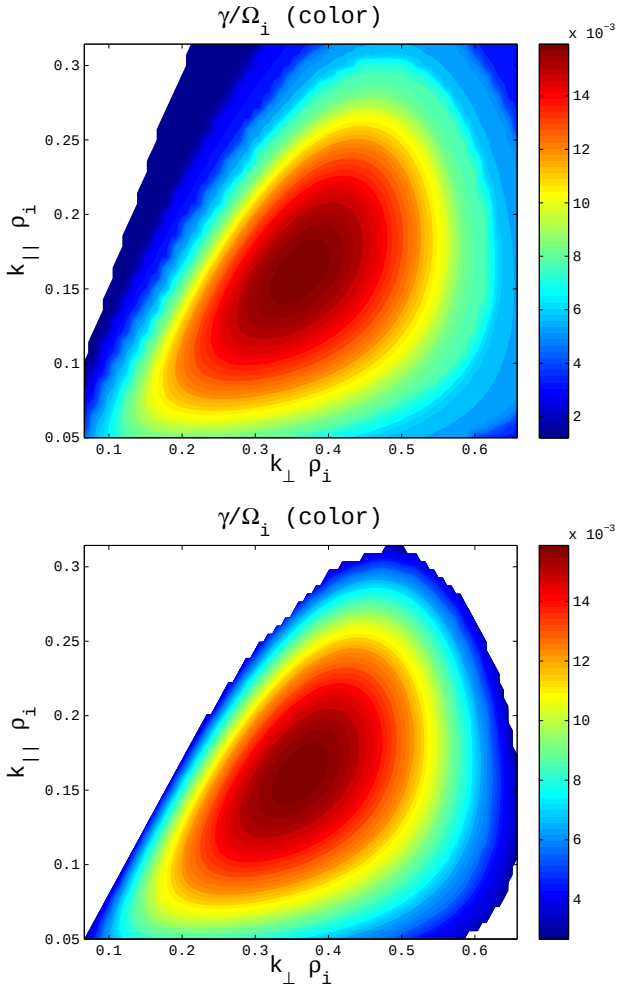

FIG. 1. Left panel shows the growth rate of the mirror instability obtained using the numerical solution of the gyrokinetic dispersion relation. The right panel shows the fully kinetic solution. The parameters were $R = 6$, $\beta_\perp = 0.43$ for ions, and electrons were isotropic with $T_e/T_i = 10^{-4}$.

Like the classical firehose, which propagates along the magnetic field[11], the oblique firehose instability requires that the parallel temperature of the unstable species be larger than the perpendicular temperature, specifically

$$N + \sum_s \beta_{s\perp}\left(1 - \frac{T_{s\parallel}}{T_{s\perp}}\right) < 0, \tag{26}$$

for some positive number N. For classical firehose $N = 2$, but for the oblique firehose $N \sim 1.4$[12]. The stability threshold for the latter is therefore slightly less, suggesting that it may be more important at controlling anisotropy near marginal stability. Furthermore, unlike the classical firehose, the maximum growth rate for the oblique firehose occurs at

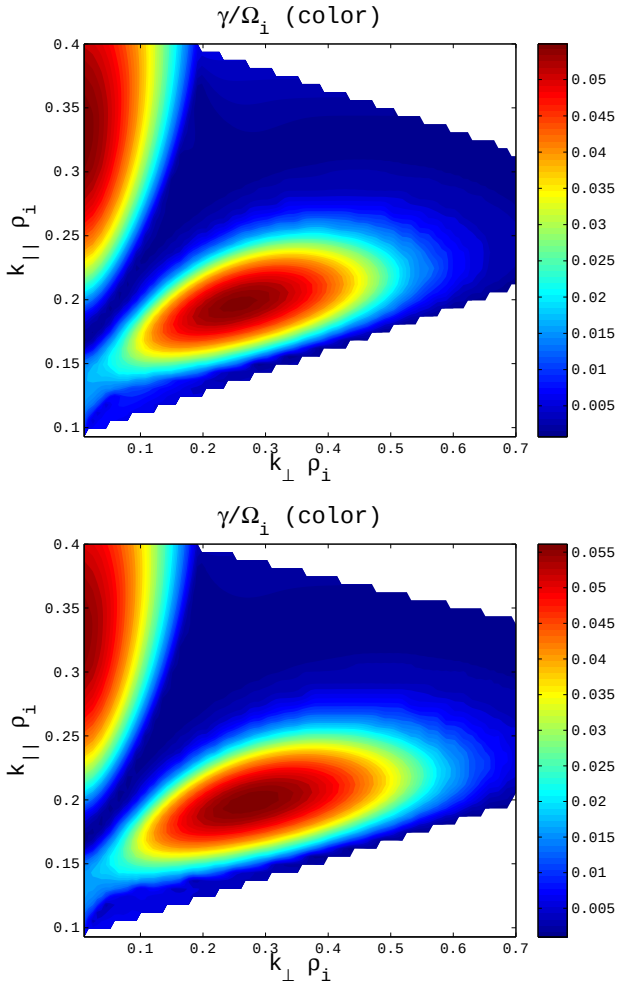

FIG. 2. Left panel shows the growth rate of the oblique firehose obtained using the numerical solution of the gyrokinetic dispersion relation. The right panel shows the fully kinetic solution. The parameters were $R = 0.4$, $\beta_\perp = 1.2$ for ions, and electrons were isotropic with $T_e/T_i = 10^{-4}$.

$k_\parallel \sim k_\perp$. This property is again the reason why this instability can not be recovered in the framework of low frequency gyrokinetics, for which $\omega/\Omega_i \ll 1$, while $k_\perp \rho_{i\perp} \sim 1$. The left panel of Figure 2 shows the dispersion surface for the oblique firehose where the ions were treated gyrokinetically, with parameters $R = 0.4$, and $\beta_\perp = 1.2$, and electrons were isotropic with $T_e/T_i = 10^{-4}$ The right panel shows the growth rate as obtained from the fully kinetic theory. The slight shift in the location of the maximum growth rate is a result of keeping only $n = \pm 1$ cyclotron resonances in the gyrokinetic solution. The proton resonant firehose instability[9], or the whistler firehose[12], is also visible.

V. DISCUSSION

The conductivity tensor for a two-component plasma, with bi-Maxwellian protons and Maxwellian electrons, has been derived above using the gyro-gauge kinetic formalism, without frequency ordering, but retaining only $n = \pm 1$ proton cyclotron resonances. The mirror and the oblique firehose instabilities were recovered by numerically solving the dispersion relation derived from the gyrokinetic plasma response, and the results agree well with fully kinetic solutions. Because no assumtion was made on wave frequency with respect to the cyclotron frequency, the result can be considered to be an alternative way to derive the fully kinetic conductivity tensor for a magnetized, bi-Maxwellian plasma, by retaining all harmonics of the cyclotron frequency, $n = -\infty, ..., \infty$. Equivalently, one may obtain quantitatively same matrix elements of the conductivity tensory by retaining only the $n = \pm 1$ cyclotron harmonics in the fully kinetic expressions found in the literature, such as *Stix* [36] or *Swanson* [37]. The significance of this approach lies, however, mainly in its implications for kinetic simulations. The approach allows one to systematically manipulate time-scales retained in the simulation model without the need to significantly alter the simulation model, or the simulation code. This flexibility is realized through suitable approximation of the gyro-gauge function, which contains all information about the transformation between particles and guiding centers[28]. How much detail is retained in the simulation model is therefore governed, in a mathematically rigorous and transparent way, by how much detail is retained in the gyro-gauge function.

Appendix A: Explicit Form of the FLR Current Components

The explicit form of the current components is given here for completeness. Combining Eq. 12 with Eq. 20 the following expressions for the components of $\mathbf{J}^{FLR}$ may be obtained,

$$\begin{aligned}
J_x^{FLR} =& \frac{\delta\phi e^{-\lambda}}{\sqrt{2}\lambda^{3/2}k_\parallel T_{i\parallel}^{3/2}}\left\{\lambda I_1 Z_+\left(k_\parallel\zeta_+ - T_{i\parallel}\right) - \lambda I_1 Z_-\left(k_\parallel\zeta_- + T_{i\parallel}\right)\right\} \\
&+ \frac{\delta B_\parallel e^{-\lambda}}{\sqrt{2}\lambda^{3/2}k_\parallel T_{i\parallel}^{3/2}}\left\{-\lambda I_0 Z_+\left(k_\parallel\zeta_+ - T_{i\parallel}\right) + I_1 Z_+\left(k_\parallel\zeta_+ - T_{i\parallel}\right) + \lambda I_1 Z_+\left(k_\parallel\zeta_+ - T_{i\parallel}\right)\right. \\
&\left.+\lambda I_0 Z_-\left(k_\parallel\zeta_- + T_{i\parallel}\right) - I_1 Z_-\left(k_\parallel\zeta_- + T_{i\parallel}\right) - \lambda I_1 Z_-\left(k_\parallel\zeta_- + T_{i\parallel}\right)\right\} \\
&- \frac{\delta A_\parallel e^{-\lambda}}{\sqrt{2}\lambda^{3/2}k_\parallel T_{i\parallel}^{3/2}} I_1\left\{Z_+\left(1+\lambda\zeta_+\right)\left(k_\parallel\zeta_+ - T_{i\parallel}\right) + Z_-\left(1-\lambda\zeta_-\right)\left(k_\parallel\zeta_- + T_{i\parallel}\right)\right. \\
&\left.- \sqrt{2T_{i\parallel}}k_\parallel\lambda\left(\zeta_- - \zeta_+\right) - 2^{3/2}\sqrt{T_{i\parallel}}\left(\lambda T_{i\parallel} - k_\parallel\right)\right\}, \qquad \text{(A1)}
\end{aligned}$$

$$\begin{aligned}
J_y^{FLR} =& \frac{i\delta\phi e^{-\lambda}}{\sqrt{2}\lambda^{3/2}k_\parallel T_{i\parallel}^{3/2}}\left\{\lambda^2 I_0 Z_+\left(k_\parallel\zeta_+ - T_{i\parallel}\right) - \lambda(1+\lambda) I_1 Z_+\left(k_\parallel\zeta_+ - T_{i\parallel}\right) + 2\sqrt{2}\lambda^2 k_\parallel I_0\sqrt{T_{i\parallel}}\right. \\
&\left.-2\sqrt{2}\lambda k_\parallel I_1\sqrt{T_{i\parallel}} - 2\sqrt{2}\lambda^2 k_\parallel I_1\sqrt{T_{i\parallel}} + \lambda^2 I_0 Z_-\left(k_\parallel\zeta_- + T_{i\parallel}\right) - \lambda(1+\lambda) I_1 Z_-\left(k_\parallel\zeta_- + T_{i\parallel}\right)\right\} \\
&+ \frac{i\delta B_\parallel e^{-\lambda}}{\sqrt{2}\lambda^{3/2}k_\parallel T_{i\parallel}^{3/2}}\left\{2\lambda^2 I_0 Z_+\left(k_\parallel\zeta_+ - T_{i\parallel}\right) + \left(-1-2\lambda-2\lambda^2\right) I_1 Z_+\left(k_\parallel\zeta_+ - T_{i\parallel}\right)\right. \\
&+2\sqrt{2}k_\parallel T_{i\parallel}^{3/2}\left(-\lambda^2 I_0 + (1+\lambda)^2 I_1\right) + 4\sqrt{2}\lambda^2 k_\parallel I_0\sqrt{T_{i\parallel}} - 2\sqrt{2}k_\parallel I_1\sqrt{T_{i\parallel}} - 4\sqrt{2}\lambda k_\parallel I_1\sqrt{T_{i\parallel}} \\
&\left.-4\sqrt{2}\lambda^2 k_\parallel I_1\sqrt{T_{i\parallel}} + 2\lambda^2 I_0 Z_-\left(k_\parallel\zeta_- + T_{i\parallel}\right) + \left(-1-2\lambda-2\lambda^2\right) I_1 Z_-\left(k_\parallel\zeta_- + T_{i\parallel}\right)\right\} \\
&+ \frac{i\delta A_\parallel e^{-\lambda}}{\sqrt{2}\lambda^{3/2}T_{i\parallel}^{3/2}}\left(I_1 + \lambda I_1 - \lambda I_0\right)\left\{\left(k_\parallel\zeta_+ - T_{i\parallel}\right)\left(\frac{\lambda}{k_\parallel}Z_+\zeta_+ + Z_+\right)\right. \\
&\left.+ \left(k_\parallel\zeta_- + T_{i\parallel}\right)\left(\frac{\lambda}{k_\parallel}Z_-\zeta_- - Z_-\right) + \sqrt{2T_{i\parallel}}\lambda\left(\zeta_- + \zeta_+\right)\right\}, \qquad \text{(A2)}
\end{aligned}$$

$$
\begin{aligned}
J_z^{FLR} = & -\frac{\delta\phi e^{-\lambda}}{2\lambda k_\parallel T_{i\parallel}^{3/2}}\Big\{\sqrt{2}\lambda I_1 Z_+\zeta_+\left(k_\parallel\zeta_+ - T_{i\parallel}\right) + 2bk_\parallel I_1\zeta_-\sqrt{T_{i\parallel}} + 2\lambda k_\parallel I_1\zeta_+\sqrt{T_{i\parallel}} \\
& +\sqrt{2}\lambda I_1 Z_-\zeta_-\left(k_\parallel\zeta_- + T_{i\parallel}\right)\Big\} - \frac{\delta B_\parallel e^{-\lambda}}{2\lambda k_\parallel T_{i\parallel}^{3/2}}\Big\{-\sqrt{2}\lambda I_0 Z_+\zeta_+\left(k_\parallel\zeta_+ - T_{i\parallel}\right) + \sqrt{2}I_1 Z_+\zeta_+\left(k_\parallel\zeta_+ - T_{i\parallel}\right) \\
& +\sqrt{2}\lambda I_1 Z_+\zeta_+\left(k_\parallel\zeta_+ - T_{i\parallel}\right) - 2\lambda k_\parallel I_0\zeta_-\sqrt{T_{i\parallel}} + 2k_\parallel I_1\zeta_-\sqrt{T_{i\parallel}} + 2\lambda k_\parallel I_1\zeta_-\sqrt{T_{i\parallel}} - 2\lambda k_\parallel I_0\zeta_+\sqrt{T_{i\parallel}} \\
& +2k_\parallel I_1\zeta_+\sqrt{T_{i\parallel}} + 2\lambda k_\parallel I_1\zeta_+\sqrt{T_{i\parallel}} - \sqrt{2}\lambda I_0 Z_-\zeta_-\left(k_\parallel\zeta_- + T_{i\parallel}\right) + \sqrt{2}I_1 Z_-\zeta_-\left(k_\parallel\zeta_- + T_{i\parallel}\right) \\
& +\sqrt{2}\lambda I_1 Z_-\zeta_-\left(k_\parallel\zeta_- + T_{i\parallel}\right)\Big\} \\
& + \frac{\delta A_\parallel e^{-\lambda}}{\sqrt{2}\lambda T_{i\parallel}^{3/2}k_\parallel} I_1\left\{\left(k_\parallel\zeta_+ - T_{i\parallel}\right)\left(2Z_+\zeta_+ + \sqrt{2T_{i\parallel}}\right)\left(\lambda\zeta_+ + k_\parallel\right)\right. \\
& \left. + \left(k_\parallel\zeta_- + T_{i\parallel}\right)\left(2Z_-\zeta_- + \sqrt{2T_{i\parallel}}\right)\left(\lambda\zeta_- - k_\parallel\right) + \left(k_\parallel\zeta_+ - T_{i\parallel}\right)\sqrt{2T_{i\parallel}}k_\parallel - \left(k_\parallel\zeta_- + T_{i\parallel}\right)\sqrt{2T_{i\parallel}}k_\parallel\right\}
\end{aligned}
\tag{A3}
$$

where $Z = Z\left(\frac{s}{\sqrt{2T_{i\parallel}}}\right)$, $\zeta_\pm = \frac{\omega \pm 1}{k_\parallel}$, $Z_\pm = Z\left(\frac{\zeta_\pm}{\sqrt{2T_{i\parallel}}}\right)$.

REFERENCES

[1]Bale, S. D., J. C. Kasper, G. G. Howes, E. Quataert, C. Salem, and D. Sundkvist (2009), Magnetic Fluctuation Power Near Proton Temperature Anisotropy Instability Thresholds in the Solar Wind, *Physical Review Letters*, *103*(21), 211,101, doi: 10.1103/PhysRevLett.103.211101.

[2]Brizard, A. (1990), Nonlinear gyrokinetic tokamak physics, Ph.D. thesis, Princeton University.

[3]Brizard, A. J., and T. S. Hahm (2007), Foundations of nonlinear gyrokinetic theory, *Rev. Mod. Phys.*, *79*(2), 421–468, doi:10.1103/RevModPhys.79.421.

[4]Califano, F., P. Hellinger, E. Kuznetsov, T. Passot, P. L. Sulem, and P. M. Trávníček (2008), Nonlinear mirror mode dynamics: Simulations and modeling, *Journal of Geophysical Research (Space Physics)*, *113*, 8219, doi:10.1029/2007JA012898.

[5]Chen, L., and S.-T. Tsai (1983), Linear oscillations in general magnetically confined plasmas, *Plasma Physics*, *25*(4), 349.

[6]Chiu, S. C. (1985), Application of the gyrokinetic equation to high frequency rf, *Plasma Physics and Controlled Fusion*, *27*(12B), 1525.

[7]Dettrick, S., L. jin Zheng, and L. Chen (2003), Kinetic theory of geomegantic pulsations: 4. Hybrid gyrokinetic simulation of drift-bounce resonant excitation of shear Alfven waves, *J. Geophys. Res.*, *108*, 1150, doi:10.1029/2002JA009650.

[8]Gary, S. P. (2015), Short-wavelength plasma turbulence and temperature anisotropy instabilities: recent computational progress, *Philosophical Transactions of the Royal Society of London Series A*, *373*, 20140,149–20140,149, doi:10.1098/rsta.2014.0149.

[9]Gary, S. P., H. Li, S. O'Rourke, and D. Winske (1998), Proton resonant firehose instability: Temperature anisotropy and fluctuating field constraints, *Journal of Geophysical Research*, *103*, 14,567–14,574, doi:10.1029/98JA01174.

[10]Hasegawa, A. (1969), Drift mirror instability in the magnetosphere, *Physics of Fluids*, *12*(12), 2642–2650, doi:10.1063/1.1692407.

[11]Hasegawa, A. (1971), Plasma instabilities in the magnetosphere, *Rev. Geophys.*, *9*, 703–772.

[12]Hellinger, P., and H. Matsumoto (2000), New kinetic instability: Oblique Alfvén fire hose, *Journal of Geophysical Research*, *105*, 10,519–10,526, doi:10.1029/1999JA000297.

[13]Hellinger, P., and P. M. Trávníček (2008), Oblique proton fire hose instability in the expanding solar wind: Hybrid simulations, *Journal of Geophysical Research (Space Physics)*, *113*, A10109, doi:10.1029/2008JA013416.

[14]Hellinger, P., and P. M. Trávníček (2015), Proton temperature-anisotropy-driven instabilities in weakly collisional plasmas: Hybrid simulations, *Journal of Plasma Physics*, *81*(1), 305810103, doi:10.1017/S0022377814000634.

[15]Hellinger, P., P. Trávníček, J. C. Kasper, and A. J. Lazarus (2006), Solar wind proton temperature anisotropy: Linear theory and WIND/SWE observations, *Geophys. Res. Lett.*, *33*, L09101, doi:10.1029/2006GL025925.

[16]Jian Liu, Z. Y., and H. Qin (2014), A nonlinear pic algorithm for high frequency waves in magnetized plasmas based on gyrocenter gauge kinetic theory, *Commun. Comput. Phys.*, *15*, 1167.

[17]Kasper, J. C., A. J. Lazarus, and S. P. Gary (2002), Wind/SWE observations of firehose constraint on solar wind proton temperature anisotropy, *Geophys. Res. Lett.*, *29*, 1839, doi:10.1029/2002GL015128.

[18]Klein, K. G., and G. G. Howes (2015), Predicted impacts of proton temperature anisotropy on solar wind turbulence, *Physics of Plasmas*, *22*(3), 032903, doi:10.1063/1.4914933.

[19]Kolesnikov, R. A., W. W. Lee, H. Qin, and E. Startsev (2007), High Frequency Gyrokinetic Particle-in-Cell Simulation: Application to Heating of Magnetically Confined Plasmas, in *Radio Frequency Power in Plasmas*, *American Institute of Physics Conference Series*, vol. 933, edited by P. Ryan and D. Rasmussen, pp. 475–478.

[20]Kolesnikov, R. A., W. W. Lee, H. Qin, and E. Startsev (2007), High frequency gyrokinetic particle simulation, *Physics of Plasmas*, *14*(7), 072,506, doi:10.1063/1.2751600.

[21]Kolesnikov, R. A., W. W. Lee, and H. Qin (2008), Electromagnetic high frequency gyrokinetic particle-in-cell simulation., *Commun. Comput. Phys*, *4*, 575–591.

[22]Lee, X. S., J. R. Myra, and P. J. Catto (1983), General frequency gyrokinetics, *Physics of Fluids*, *26*, 223–229.

[23]Lin, Y., X. Wang, Z. Lin, and L. Chen (2005), A gyrokinetic electron and fully kinetic ion plasma simulation model, *Plasma Physics and Controlled Fusion*, *47*(4), 657.

[24]Numata, R., G. G. Howes, T. Tatsuno, M. Barnes, and W. Dorland (2010), AstroGK: Astrophysical gyrokinetics code, *Journal of Computational Physics*, *229*, 9347–9372, doi:10.1016/j.jcp.2010.09.006.

[25]Porazik, P., and J. R. Johnson (2013), Gyrokinetic simulation of the nonlinear evolution of mirror instability, *Journal of Geophysical Research*, *118*, 1–8, doi:10.1002/2013JA019308.

[26]Porazik, P., and J. R. Johnson (2013), Linear dispersion relation for the mirror instability in context of the gyrokinetic theory, *Physics of Plasmas*, *20*(10), 104,501, doi:10.1063/1.4822339.

[27]Porazik, P., and Z. Lin (2011), Gyrokinetic particle simulation of drift-compressional modes in dipole geometry, *Physics of Plasmas*, *18*(7), 072,107, doi:DOI:10.1063/1.3605031.

[28]Qin, H. (1998), Gyrokinetic theory and computational methods for electromagnetic perturbations in tokamaks, Phd. thesis, Princeton University.

[29]Qin, H., and W. M. Tang (2004), Pullback transformations in gyrokinetic theory, *Physics of Plasmas*, *11*(3), 1052–1063, doi:10.1063/1.1640626.

[30]Qin, H., W. M. Tang, W. W. Lee, and G. Rewoldt (1999), Gyrokinetic perpendicular dynamics, *Physics of Plasmas*, *6*(5), 1575–1588, doi:10.1063/1.873411.

[31]Qin, H., C. K. Phillips, R. A. Kolesnikov, W. W.-L. Lee, E. J. Valeo, and D. N. Smithe (2007), Gyrocenter Gauge Theory and Algorithm for Nonlinear Particle Simulations of Radio-Frequency Waves in Plasmas, in *Radio Frequency Power in Plasmas*, *American Institute of Physics Conference Series*, vol. 933, edited by P. Ryan and D. Rasmussen, pp.

471–474.

[32]Qu, H., Z. Lin, and L. Chen (2007), Gyrokinetic theory and simulation of mirror instability, *Physics of Plasmas*, *14*(4), 042,108, doi:10.1063/1.2721074.

[33]Qu, H., Z. Lin, and L. Chen (2008), Nonlinear saturation of mirror instability, *Geophys. Res. Lett.*, *35*(10), L10,108.

[34]Seough, J., P. H. Yoon, and J. Hwang (2015), Simulation and quasilinear theory of proton firehose instability, *Physics of Plasmas*, *22*(1), 012303, doi:10.1063/1.4905230.

[35]Southwood, D. J., and M. G. Kivelson (1993), Mirror instability: 1. Physical mechanism of linear instability, *Journal of Geophysical Research*, *98*, 9181–9187.

[36]Stix, T. H. (1992), *Waves in Plasmas*, Springer-Verlag.

[37]Swanson, D. G. (1989), *Plasma Waves*, Academic Press, San Diego, ch. 6.

[38]Tajiri, M. (1967), Propagation of hydromagnetic waves in collisionless plasma. ii. kinetic approach, *Journal of the Physical Society of Japan*, *22*(6), 1482–1494, doi:10.1143/JPSJ.22.1482.

[39]Told, D., F. Jenko, J. M. TenBarge, G. G. Howes, and G. W. Hammett (2015), Multi-scale Nature of the Dissipation Range in Gyrokinetic Simulations of Alfvénic Turbulence, *Physical Review Letters*, *115*(2), 025003, doi:10.1103/PhysRevLett.115.025003.

[40]Yoon, P. H., C. S. Wu, and A. S. de Assis (1993), Effect of finite ion gyroradius on the fire-hose instability in a high beta plasma, *Physics of Fluids B*, *5*, 1971–1979, doi:10.1063/1.860785.

[41]Yoon, P. H., J. Seough, J. Hwang, and Y. Nariyuki (2015), Macroscopic quasi-linear theory and particle-in-cell simulation of helium ion anisotropy instabilities, *Journal of Geophysical Research (Space Physics)*, *120*, 6071–6084, doi:10.1002/2015JA021495.

[42]Yu, Z., and H. Qin (2009), Gyrocenter-gauge kinetic algorithm for high frequency waves in magnetized plasmas, *Physics of Plasmas*, *16*(3), 032,507, doi:10.1063/1.3097266.

PPPL PRINCETON PLASMA PHYSICS LABORATORY

Princeton Plasma Physics Laboratory
Office of Reports and Publications

Managed by
Princeton University

under contract with the
U.S. Department of Energy
(DE-AC02-09CH11466)

P.O. Box 451, Princeton, NJ 08543
Phone: 609-243-2245
Fax: 609-243-2751

E-mail: publications@pppl.gov

Website: http://www.pppl.gov